J Mater Sci (2018) 53:5467–5476

Polymers

Poly(NIPAAm-*co*-Ru(bpy)$_3^{2+}$) hydrogels crosslinked by double-bond end-capped Pluronic F127: preparation, properties and coupling with the BZ reaction

Hongwei Zhou[1,*], Bo Yan[1], Jie Li[2], Hanbin Liu[3], Qiang Wang[1], Xiaobin Ding[2], Xilang Jin[1,*], Aijie Ma[1], Weixing Chen[1], Jingjing Yang[1], Chunyan Luo[1], Gai Zhang[1], and Weifeng Zhao[1]

[1] *School of Materials and Chemical Engineering, Xi'an Technological University, Xi'an 710021, People's Republic of China*
[2] *Chengdu Institute of Organic Chemistry, University of Chinese Academy of Sciences, Chengdu 610041, People's Republic of China*
[3] *School of Bioresources Chemical and Materials Engineering, Shaanxi University of Science and Technology, Xi'an 710021, People's Republic of China*

Received: 20 September 2017
Accepted: 12 December 2017
Published online: 19 December 2017

ABSTRACT

Topological network design is an effective way to obtain new functionalities and regulate the properties of stimuli responsive hydrogels. In this work, poly(NIPAAm-*co*-Ru(bpy)$_3^{2+}$) hydrogels (NIPAAm: *N*-isopropylacrylamide, Ru(bpy)$_3^{2+}$: Ruthenium bipyridine complex monomer) crosslinked by amphiphilic triblock copolymers were designed and constructed by a photo-induced gelation method, utilizing double-bond end-capped Pluronic F127 (F127DA) as the crosslinking agent, NIPAAm and Ru(bpy)$_3^{2+}$ as the monomers, α-ketoglutaric acid as the photoinitiator and H_2O as the solvent. The resulting F127DA crosslinked hydrogels exhibit unique swelling behaviors, mechanical properties, fluorescent behaviors and thermosensitive properties and can be coupled with the BZ reaction. The present example may enrich the family of metal-containing polymer materials and provide clues to develop other functional hydrogels by designing topologically crosslinked network.

Introduction

Stimuli responsive hydrogels are three-dimensionally crosslinked networks that can dramatically respond to various external stimuli, including temperature, pH, light, small molecules and electric field [1–3]. Different from linear polymers, stimuli responsive hydrogels can be swollen by absorbing large amount of water but cannot be completely dissolved. The unique structure, properties and responsive behaviors make stimuli responsive hydrogels versatile candidate materials for tissue engineering, sensors,

Address correspondence to E-mail: xatuzhou@163.com; jinxilang_911@163.com

https://doi.org/10.1007/s10853-017-1929-1

artificial muscles, soft robots, controlled valves and separations [4–11].

Inspired by the self-oscillating phenomena in nature, such as heartbeat, brain waves, pulsatile secretion of hormones and biorhythms, autonomously responsive hydrogels, so-called the self-oscillating hydrogels (SOHs), are designed and constructed [12–16]. In such hydrogel systems, the stimuli factors that are generated in chemical oscillating reactions show autonomous, reversible and periodical variation [16]. The self-oscillation of stimuli factors drives the self-regulated behaviors of polymer materials without any "ON/OFF" switching of external stimuli. A generally utilized strategy is based on the coupling of hydrogels with the Belousov–Zhabotinsky (BZ) reactions via the covalently bonded organometallic catalysts [e.g., $Ru(bpy)_3^{2+}$] in polymer chains [17]. The occurrence of the BZ reactions in the hydrogel networks leads to an autonomous redox variation of the ruthenium complex between $Ru(bpy)_3^{2+}$ and $Ru(bpy)_3^{3+}$ and induces an autonomous expansion–shrinkage transformation of the hydrogels [18].

Topological structure design is an effective way to improve the properties and to extend the options of SOHs [14, 19, 20]. Suzuki and coworkers demonstrated that hierarchically structured SOHs assembled from self-oscillating submicron-sized hydrogel particles (microgels) showed better properties than the traditional *N*,*N*′-methylenebisacrylamide (MBA) crosslinked counterparts [21]. The hierarchical hydrogels were prepared by a two-step method. First, the microgels were first prepared by a free radical precipitation polymerization utilizing NIPAAm, $Ru(bpy)_3^{2+}$ monomers and *N*-(3-aminopropyl)methacrylamide hydrochloride (APMA) as the monomers and MBA as the crosslinking agent. Second, the obtained microgels were covalently crosslinked using glutaric dialdehyde to obtain the target hierarchical hydrogels. In such hierarchical network, both the microgel units and the bulk SOHs self-oscillate along with the BZ reaction and large deformation can be observed. Interestingly, comb-like self-oscillating hydrogels are also demonstrated to have an excellent responding rate and a large self-oscillating amplitude [22]. In such SOHs, $Ru(bpy)_3^{2+}$ groups are introduced in both the main chains and the side chains. Because the side polymer chains are not crosslinked and can freely move and interact with the substances of the BZ reaction, the comb-like SOHs show faster and larger swelling/deswelling compared with the traditional SOHs. Another example by Epstein and Xu verified that $Ru(bpy)_3^{2+}$-derived multifunctional complexes containing six polymerizable double bonds in the bipyridine ligands can work as both hyper-crosslinker and catalysts of the BZ reaction [23]. The unique topological structure leads to an inverted volume transition behavior that is different from the traditionally MBA crosslinked SOHs. In our previous work, introduction of special crosslinking points, for instance polyrotaxane, was demonstrated as efficient ways to construct functional hydrogels [24–26]. Although much effort has been made to obtain SOHs by designing unique network structure, the mechanical robustness, oscillation amplitude and options of SOHs are still limited [17, 27].

Herein, we aim at designing and preparing novel topologically crosslinked poly(NIPAAm-*co*-$Ru(bpy)_3^{2+}$) hydrogels by utilizing amphiphilic triblock copolymers as the crosslinking agents. Due to the amphiphilic nature, the copolymers can self-assemble into micellar aggregates in their aqueous solutions. Compared with the MBA crosslinking agents, the copolymer micelle crosslinking points can promote flexible dislocation along with the chain slippage and bring new structure and properties to hydrogels. In detail, double-bond end-capped Pluronic F127 (F127DA) was selected, in which polyethylene oxide (PEO) is the hydrophilic segment and polypropylene oxide (PPO) works as the hydrophobic part. Therefore, F127DA forms micelles containing vinyl groups on the surface, which work as chemical crosslinking points. The target F127DA crosslinked hydrogels are prepared in water utilizing F127DA as the crosslinking agents, NIPAAm and $Ru(bpy)_3^{2+}$ as the monomers and α-ketoglutaric acid as the photoinitiator. The resulting hydrogels exhibit unique swelling behaviors, mechanical properties, fluorescent behaviors and thermosensitive properties and can be coupled with the BZ reaction.

Experimental

Materials

α-ketoglutaric acid (A.R.), Pluronic F127 (M_n: 10,000–12,000 g mol^{-1}), acryloyl chloride (97%) and NIPAAm were purchased from Energy Chemical. NIPAAm was purified by recrystallization before

use. $Ru(bpy)_3$ monomer was prepared and purified according to the previous method [18].

Synthesis

F127DA was firstly synthesized according to the previously established method [25, 26, 28]. In a typical run, the preparation procedure of F127DA crosslinked hydrogels was as follows. A 2 mL aqueous solution of NIPAAm (1.38 mol/L), $Ru(bpy)_3$ (0.0022 mol/L), and F127DA (0.36%, molar feed ratio to monomers of NIPAAm and $Ru(bpy)_3$) was firstly prepared and bubbled with N_2 for 30 min. Then, α-ketoglutaric acid (0.2 wt%) was added and the resulting solution was injected into a glass mold separated by a 4-mm silicone rubber sheet. Then, the gelation system was illuminated with UV light (intensity ~ 70 mW/cm^2) for 30 min. Afterward, the unreacted monomers and linear polymers were removed by dialysis against DMSO and H_2O to obtain the target F127DA crosslinked hydrogels. When the molar feed ratios of F127DA to the monomers were fixed at 0.36, 0.72 and 1.44%, the hydrogels were labeled as H1, H2 and H3, respectively.

Characterization

Scanning electron microscopy (SEM) images were captured on a Philips (Quanta 400F) system. Hydrogel samples were freeze-dried and then sputter-coated with gold in vacuum. Swelling behaviors were studied by analyzing the perimeter variation of a dried hydrogel sheet over time. The swelling ratio (SR) was calculated according to the formula of $SR = (P_i - P_0)/P_0$, where P_i is the perimeter of the hydrogel in swollen state and P_0 is the perimeter of dried hydrogel sheet. Dynamic mechanical properties analysis of the hydrogels was carried out by using an Anton Paar Physica MCR 302 rheometer equipped with a thermostatic system. UV–Vis spectra of $Ru(bpy)_3^{2+}$ monomer were recorded in its ethanol solution on a spectrophotometer (Shimadzu, UV-2550) at room temperature. Fluorescent spectra were collected on a PerkinElmer LS 55 spectrometer. Thermosensitive behaviors of hydrogels were investigated by analyzing the perimeter variation of hydrogel sheets with the increasing temperature. Hydrogel perimeters were calculated from the corresponding images which were captured on a microscope system (Olympus, CX31) equipped with a thermostatic circulator system (Yuhua, DFY-5/10). Coupling of the hydrogels with the BZ reaction was conducted on a homemade system which is composed of a glass reactor, a microscope, a CCD system and a thermostatic circulator system. A jacket was made outside of the glass reactor to connect to the thermostatic circulator system. The glass reactor was placed under the microscope for image taking and video recording.

Results and discussion

Preparation of the F127DA crosslinked hydrogels

To obtain the target F127DA crosslinked poly(NIPAAm-*co*-$Ru(bpy)_3^{2+}$) hydrogels, a photo-induced gelation process was carried out according to the procedure shown in Scheme 1. The hydrogels were prepared without addition of any other small molecular crosslinkers. The feed ratio of F127DA was varied to prepare hydrogels with

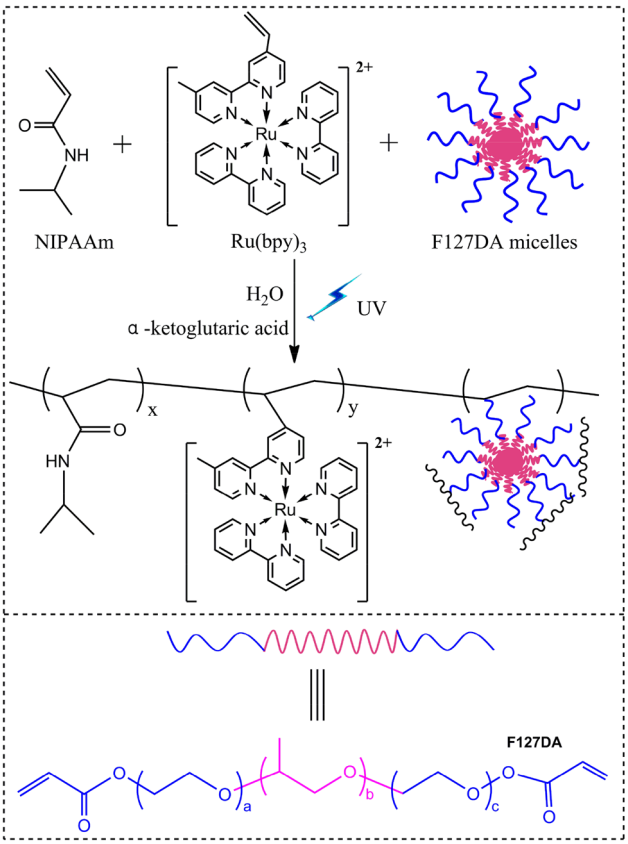

Scheme 1 Preparation route and chemical structure of the poly(NIPAAm-*co*-$Ru(bpy)_3^{2+}$) hydrogels crosslinked by F127DA.

different structures, which are labeled as H1, H2 and H3 with the increasing feed ratio of F127DA.

Swelling behaviors and the fracture surface morphology of the F127DA crosslinked hydrogels

Swelling properties and the fracture surface morphology of poly(NIPAAm-*co*-Ru(bpy)$_3^{2+}$) hydrogels were first investigated. The as-prepared F127DA crosslinked hydrogel was in its reduced state (Fig. 1a). After immersing into water, the hydrogel swelled to almost two times of its original size, indicating the good swelling property. In the equilibrium swelling state, the hydrogel shows well transparency, as revealed in Fig. 1b. The letters behind the swollen hydrogel can be clearly seen. SEM image shown in Fig. 1c indicates a porous structure for the obtained hydrogel. The existence of porous structure can ensure the timely diffusion of the chemical reactants into and out of polymer network, which is critical to the coupling of the hydrogels with the BZ reaction. To gain further insights into the swelling behaviors of the F127DA crosslinked hydrogels, the swelling ratio was measured by analyzing the perimeter variation of dried hydrogels in water. Figure 1d shows the swelling ratio of H1, H2 and H3 over time. As seen, the swelling ratio of all the three dried hydrogels shows gradual increase as a function of time, indicating the intaking of water into polymer network. Interestingly, the equilibrium swelling ratio increases with the increasing feed ratio of F127DA from H1 to H3. This may be ascribed to their different crosslinking modus. When F127DA was fed in small amount, the chemical crosslinking points were the main factor to keep the network structure of the hydrogels. But with the increase in F127DA, the content of F127 components in the hydrogel was increased. Micellation and physical entanglement became the key factor for crosslinking the hydrogel. Physical crosslinking points enable the feasible chain movement and are easy to be destroyed, which leads to the high swelling ratio. This may explain why the hydrogels with higher feed ratio of F127DA tend to exhibit higher swelling ratio.

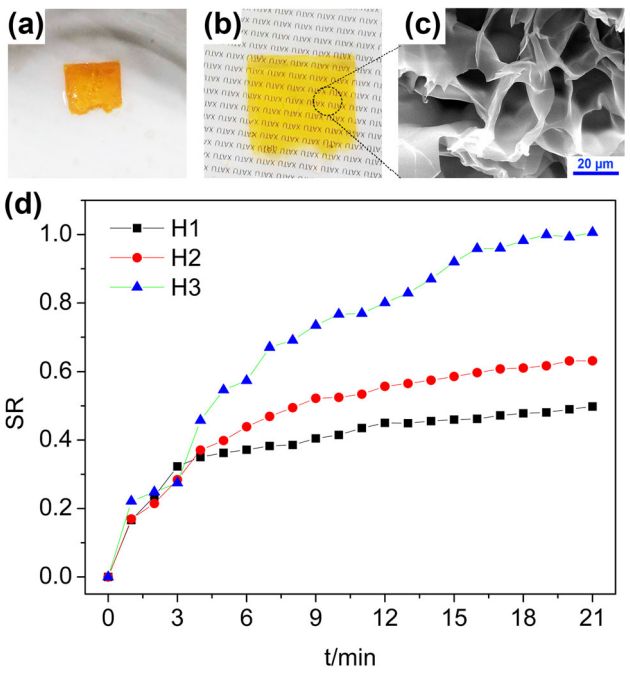

Figure 1 Swelling behaviors and structure of poly(NIPAAm-*co*-Ru(bpy)$_3^{2+}$) hydrogels crosslinked by F127DA. **a** Photographs of the hydrogel in as-prepared state. **b** In fully swollen state. **c** A typical SEM image of fracture surface of freeze-dried hydrogel. **d** Time-dependent swelling ratio curves of H1, H2 and H3.

Thermosensitive behaviors of the F127DA crosslinked hydrogels

The thermosensitive behaviors considering the redox states of Ru(bpy)$_3^{2+}$ were further investigated. Similar to other metal-containing materials, Ru(bpy)$_3^{2+}$ moieties can exhibit reversible redox variation upon external stimuli. Taking H1 as an example (Fig. 2a), the size shows gradual decrease with the increasing temperature from 15 to 55 °C in both the oxidized state (green-yellow) and the reduced state (orange). In the reduced state, the size decrease was obvious, but only slight shrinkage with the increasing temperature was observed when the Ru(bpy)$_3^{2+}$ moieties were in oxidized state. This indicates that the redox states of Ru(bpy)$_3^{2+}$ have great effects on the thermosensitive behavior of the hydrogel. The influence of feed ratio of F127DA on the thermosensitive behaviors of the hydrogels was also investigated. Figure 2b shows the photographs of fully swollen H1, H2 and H3 at 15 and 55 °C. H1 showed the most obvious thermosensitivity, as indicated by the frizzling at high temperature. In contrast, H2 showed a transparency to translucence transition when the temperature was elevated. H3 only showed a slight change in its size without observable transparence variation. This is because that PNIPAAm component plays a critical part in the thermosensitive behaviors

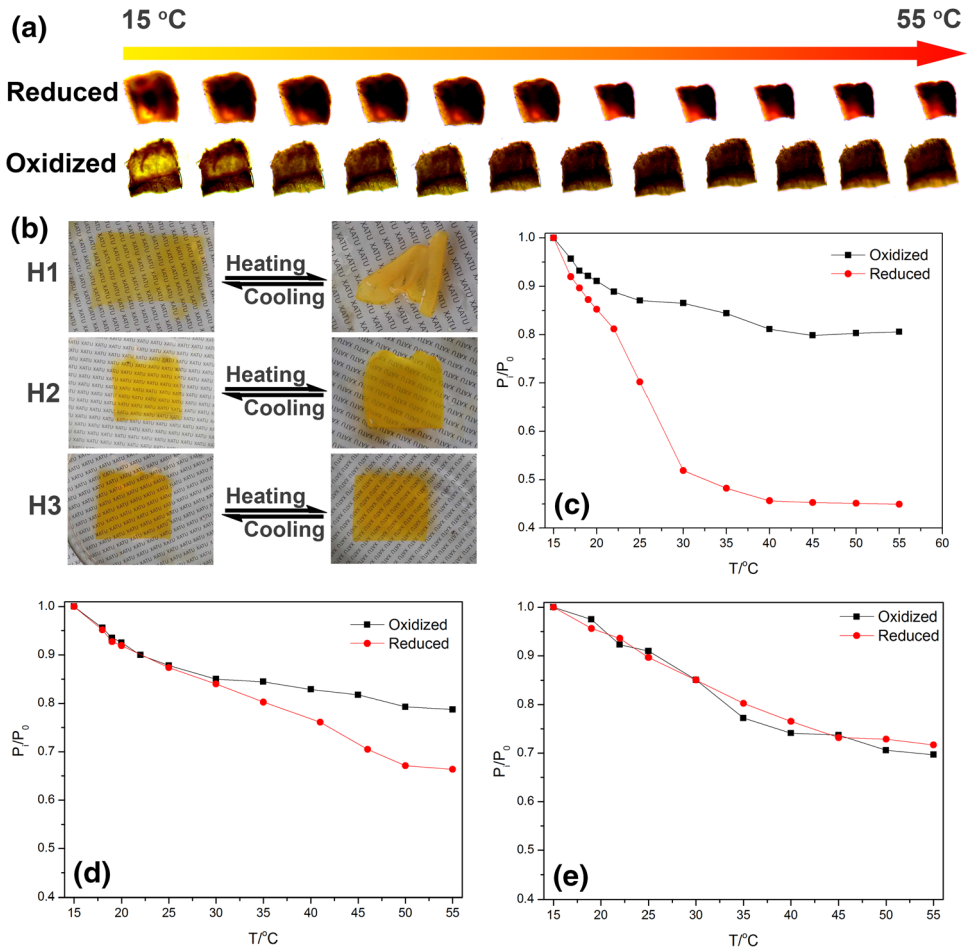

Figure 2 Thermosensitive behaviors of poly(NIPAAm-*co*-Ru(bpy)$_3^{2+}$) hydrogels crosslinked by F127DA. **a** Photographs of H1 with gradually increase in temperature from 15 to 55 °C in both the oxidized state and the reduced state. **b** Photographs of fully swollen H1, H2 and H3 at room temperature and 50 °C. **c** Temperature-dependent perimeter changes of H1 in both the oxidized state and the reduced state. **d** H2, **e** H3. P_0 is the equilibrated perimeter of the hydrogel in a solution of 3 mmol/L $Ce(SO_4)_2$ and 89.4 mmol/L HNO_3 (oxidized state) or 3 mmol/L $Ce_2(SO_4)_3$ and 89.4 mmol/L HNO_3 (reduced state) at 15 °C. P_i represents the equilibrated perimeter of the hydrogel at different temperatures.

of the hydrogels. The thermosensitivity diminishing from H1 to H3 is attributed to the decreasing content of PNIPAAm component in the hydrogels. Further quantitative investigation also showed a similar trend (Fig. 2c–e). As seen, in the case of H1, the thermosensitivity is obvious, the size change with increasing temperature is significant and the difference between the oxidized state and reduced state of the hydrogel is obvious. When the feed ratio of F127DA is increased, the thermosensitivity is limited for H2 and H3. These results could provide some clues for choosing appropriate temperature during coupling the hydrogels with the BZ reaction.

Fluorescence behaviors of the F127DA crosslinked hydrogels

Due to the existence of fluorescent Ru(bpy)$_3^{2+}$ groups, the F127DA crosslinked poly(NIPAAm-*co*-Ru(bpy)$_3^{2+}$) hydrogels are fluorescent. As shown in Fig. 3a, H1, H2 and H3 exhibit orange-red color at 25 and 50 °C under the excitation of UV light. From H1 to H3, the fluorescence intensity becomes weaker. This may be caused by the decreased content of Ru(bpy)$_3^{2+}$ moieties. Meanwhile, the relatively hydrophobic property of Ru(bpy)$_3^{2+}$ may promote cladding effects. In aqueous solution, F127DA micelles have hydrophobic microenvironment in the inner part. Part of the Ru(bpy)$_3^{2+}$ moieties are included into the micelles, and the excitation intensity of light illuminated on the Ru(bpy)$_3^{2+}$ is weakened by the shell of micelles, which leads to the decrease in the fluorescence intensity. Additional clues can be obtained from the fluorescent behaviors of Ru(bpy)$_3^{2+}$ in its solution state. Figure 3b shows that Ru(bpy)$_3^{2+}$ monomer has absorption peaks at 291 and 460 nm, which are attributed to the π–π* transition absorption and the intramolecular charge transfer absorption, respectively, indicating the successful preparation of Ru(bpy)$_3^{2+}$. Figure 3c shows that Ru(bpy)$_3^{2+}$ has a emission peak in a range of 602–613 nm in different solvents, including DMSO, DMF, ethanol and H_2O.

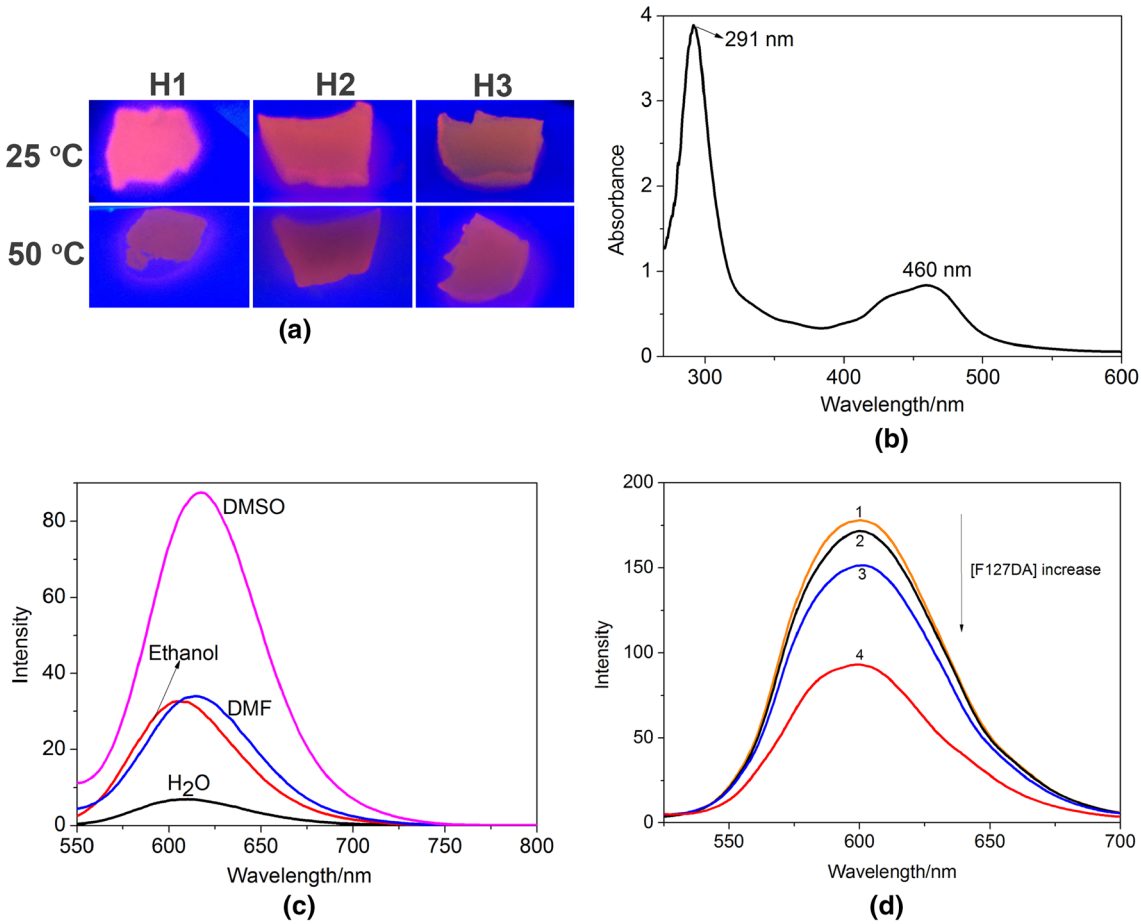

Figure 3 Fluorescent properties of poly(NIPAAm-*co*-Ru(bpy)$_3^{2+}$) hydrogels crosslinked by F127DA. **a** Photographs of H1, H2 and H3 under excitation of a UV lamp (wavelength = 365 nm) at 20 and 50 °C, respectively. **b** UV–Vis spectra of the polymerizable Ru(bpy)$_3^{2+}$ monomer (4.45 mmol/L) in ethanol. **c** Fluorescence spectra of Ru(bpy)$_3^{2+}$ monomer (4.45 mmol/L) in different solvents. **c** Fluorescence spectra of Ru(bpy)$_3^{2+}$ monomer (4.45 mmol/L) in water in the presence of F127DA with different concentrations, *1*(10 mg/mL), *2*(10.5 mg/mL), *3*(11 mg/mL) and *4*(11.5 mg/mL). The excitation wavelength is 500 nm.

The fluorescence intensity obviously decreased when the solvents changed from DMSO to DMF, ethanol and H_2O. Among these, the aqueous solution of Ru(bpy)$_3^{2+}$ showed the lowest fluorescence intensity. This may be caused by the aggregation of fluorescent molecules in their poor solvents and verifies the relatively hydrophobic nature of Ru(bpy)$_3^{2+}$. Further investigation indicates that F127DA has a remarkable influence on the fluorescent property of Ru(bpy)$_3^{2+}$. As seen from Fig. 3d, the fluorescence intensity of aqueous solution of Ru(bpy)$_3^{2+}$ shows obvious decrease with the increasing concentration of F127DA. This is in accordance with the diminishing trend of fluorescence intensity from H1 to H3. When the hydrogels were heated up to 50 °C (higher than volume phase transition temperature), H1 showed the largest shrinkage in volume and the fluorescence intensity decreased compared with that at 25 °C (Fig. 3a). The thermosensitive response of the hydrogel is originated from the PNIPAAm component. When temperature was elevated higher than the phase transition temperature, the hydrogels shrank and the fluorescent moieties Ru(bpy)$_3^{2+}$ were deeply embedded in the hydrogel network. Due to the limited transmittance of excitation light, the Ru(bpy)$_3^{2+}$ in the inner part could not be efficiently excited and the fluorescence intensity was weakened.

Viscoelastic behavior of the F127DA crosslinked hydrogels

Rheological tests were then conducted to investigate the viscoelastic behavior, mechanical properties and network evolution of the F127DA crosslinked hydrogels. Strain-controlled dynamic frequency sweep test of storage moduli (G') and loss moduli (G'') of fully swollen hydrogels from 0 to 300 rad/s was carried out as an example (Fig. 4). Compared with the previously studied MBA crosslinked hydrogels, the storage moduli and loss moduli are very small [29]. In a low frequency range below 25 rad/s, the storage moduli are higher than loss moduli, indicating that the hydrogels are self-supportive and possess a stable network (Fig. 4a–c). However, with the increase in frequency, the storage moduli become lower than loss moduli and the difference between G' and G'' increases. The signal of $G' < G''$ indicates the destruction of hydrogel networks at high frequency range, and the hydrogels start to behave like viscous liquids. The easily destructive hydrogel network is ascribed to the F127DA crosslinked structure. Because of the high molecular weight of F127DA, the ultra-long molecular chains between two chemical crosslinking points provide large free space for the micellization and physical entanglement. Compared with the covalent crosslinking points originated from double bonds at the end of F127DA, physical crosslinking points are more likely to be the critical factor for keeping the shape and mechanical properties of hydrogels. But the physical crosslinking points are easily destroyed and leads to a destruction of the network under high frequency shear force.

In order to further investigate the response of the hydrogels to temperature, dynamic mechanical tests were carried out. Figure 4d–f displays the strain-controlled dynamic frequency sweep of G' and G'' at 50 °C. For H1, G' maintains higher than G'' in the whole frequency range, which indicates that the hydrogel network of H1 at 50 °C is not easy to be destroyed as that at 20 °C. In contrast, G′ is only higher than G'' in the low frequency range and becomes lower than G′′ in high frequency range for H2 and H3. This means that H2 and H3 are not stable at 50 °C. When the temperature was elevated, additional hydrogen bonding crosslinking points formed in PNIPAAm component to enhance the hydrogel network. Therefore, H1 shows elastic response at 50 °C in the frequency range. In H2 and H3, the enhancing effects are weakened due to the low content of PNIPAAm component and the hydrogel networks are still easily destroyed when the frequency is high.

Coupling of the F127DA crosslinked hydrogels with the BZ reaction

Bridging by the $Ru(bpy)_3^{2+}$ moieties in the hydrogels, coupling of the hydrogels with the BZ reaction was achieved. This was carried out by immersing a small piece of the hydrogel into an aqueous solution of the BZ reaction substrates including HNO_3, $NaBrO_3$ and malonic acid (MA). Herein, HNO_3 provides the acidic environment, $NaBrO_3$ works as the oxidizing agent, and MA is organic acid. The BZ reaction takes place in a complicated chemical process according to the FKN mechanism with the $Ru(bpy)_3^{2+}$ on the polymer chains of the hydrogels as the catalysts [30]. The occurrence of the BZ reaction in hydrogels can be conveniently verified by the redox variation of $Ru(bpy)_3^{2+}$, during which the color changes periodically. H1, H2 and H3 were tried to couple with the BZ reaction but only H1 exhibited obvious and periodical color variation. As displayed in Fig. 5a and Video S1, the hydrogel exhibits autonomous color variation between green-yellow and orange, indicating the coupling of the hydrogel with the BZ reaction. The oscillation period from a reduced state to the next one is about 100 s. Meanwhile, the change in the red color intensity of the marked parts in the photographs over time also exhibits an oscillating profile, further indicating the occurrence of the BZ reaction (Fig. 5b). Moreover, autonomous volume oscillation was also observed when smaller H1 was coupled with the BZ reaction. Figure 5c and Video S2 show the volume change of the hydrogel over time. As seen, the volume of the hydrogel gradually decreased with the reduction process and increased with the oxidizing process. Results of analyzing the perimeters of the hydrogel also show autonomous change over time, further indicating the mechanical self-oscillation (Fig. 5d). In H2 and H3, the relatively high content of F127DA reduces the contacting chance of $Ru(bpy)_3^{2+}$ moieties with the BZ reaction substrates and leads to the failed coupling of H2 and H3 with the BZ reaction.

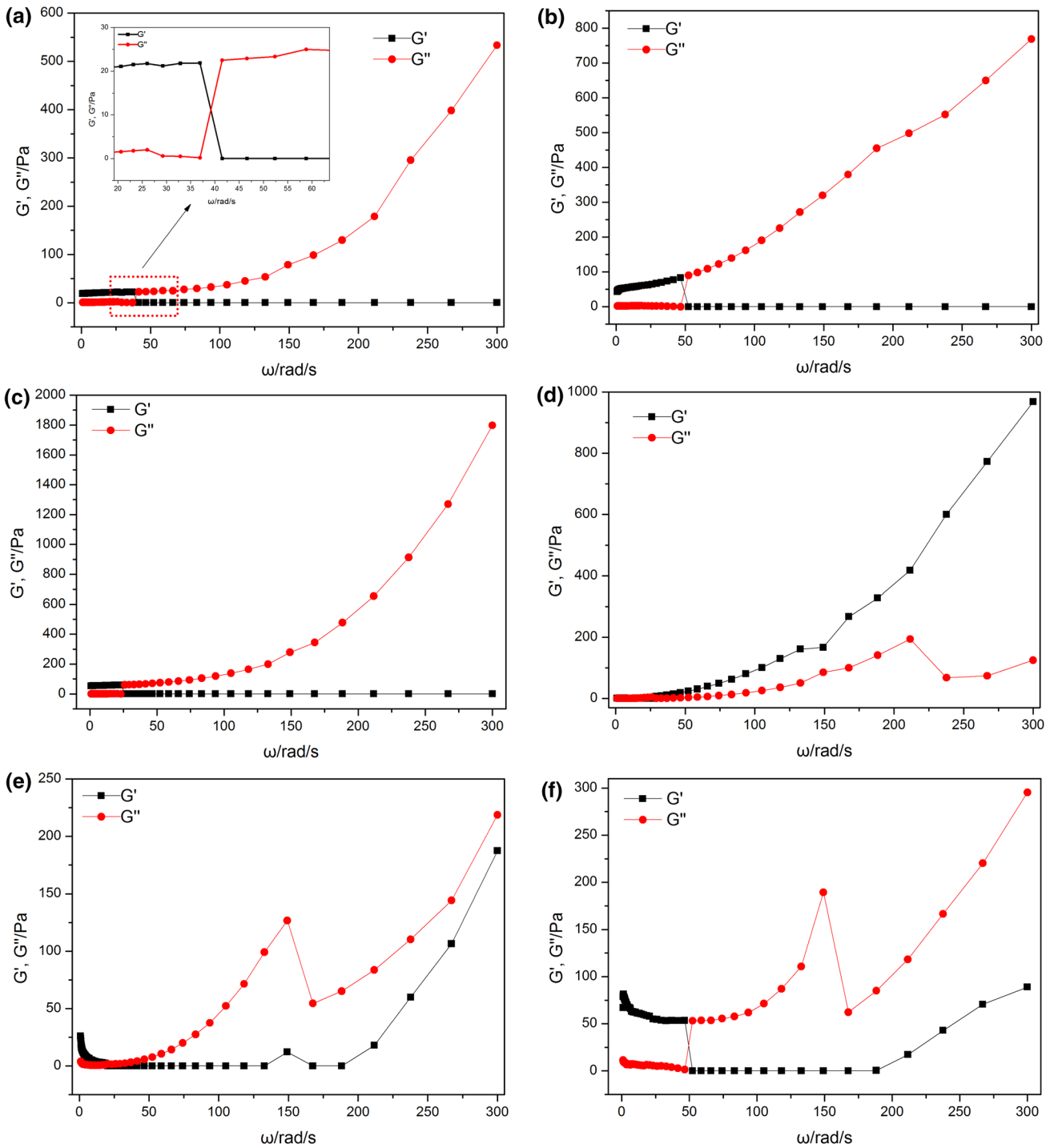

Figure 4 Rheological properties of the poly(NIPAAm-*co*-Ru(bpy)$_3^{2+}$) hydrogels crosslinked by F127DA. **a** Strain-controlled dynamic frequency sweep test of storage moduli (G') and loss moduli (G'') for H1 at 20 °C. The inset shows the amplified part from 20 rad/s to 60 rad/s. **b** H2, $T = 20$ °C, **c** H3, $T = 20$ °C, **d** H1, $T = 50$ °C, **e** H2, $T = 50$ °C, **f** H3, $T = 50$ °C. The strains for **a**–**f** were fixed at 1%.

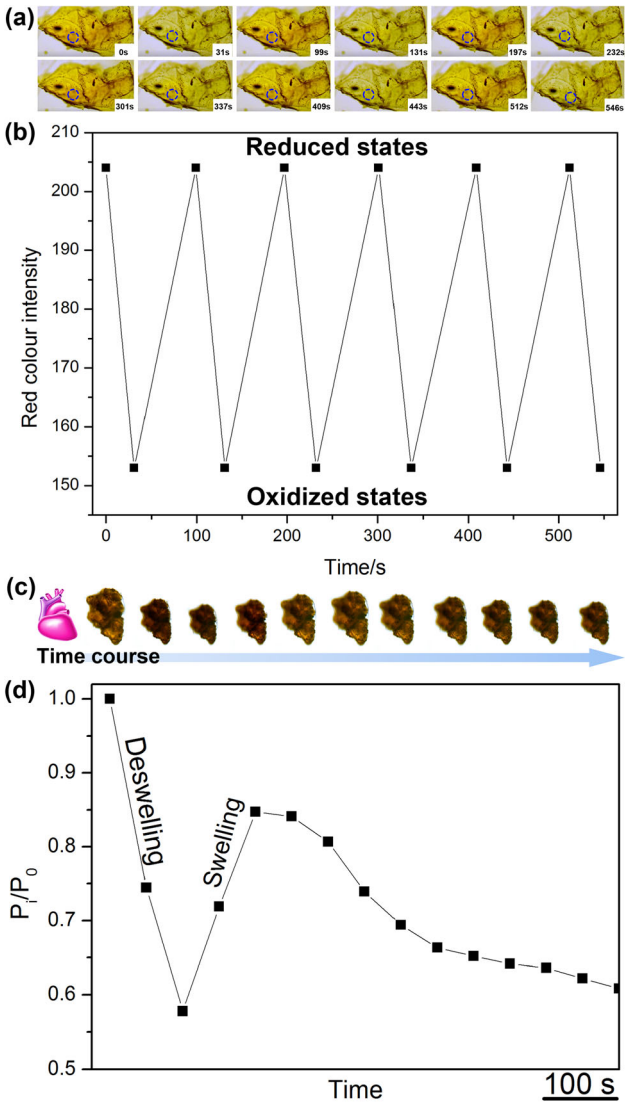

Figure 5 Coupling of the poly(NIPAAm-*co*-Ru(bpy)$_3^{2+}$) hydrogels crosslinked by F127DA with the BZ reaction. **a** Photographs of H1 (captured from Video S1) coupled with the BZ reaction. The initial conditions were fixed at [$NaBrO_3$] = 62.5 mmol/L mol/l, [malonic acid] = 84 mmol/L, [HNO_3] = 89.4 mmol/L and T = 23 °C. **b** Red color intensity variation of the marked position in **a** over time. **c** Photographs of a heart model (the first one) and heart-shaped H1 (captured from Video S2) in the BZ reaction. **d** Mechanical oscillation profiles of H1. *Pi* is the perimeter of H1 during mechanical oscillation, and P_0 is original perimeter value before volume oscillation.

Conclusions

In conclusion, poly(NIPAAm-*co*-Ru(bpy)$_3^{2+}$) hydrogels crosslinked by amphiphilic block copolymers were constructed by a photo-induced gelation method. The hydrogels exhibit unique swelling behaviors, mechanical properties, fluorescent behaviors and thermosensitive properties. Further investigation verifies that the hydrogels can also be coupled with the BZ reaction and show autonomous volume self-oscillation in the case of low feed ratio of F127DA. In a broader context, the present example not only enriches the family of metal-containing polymer materials [31, 32], but also provides clues to develop other functional hydrogels by designing topologically crosslinked network structure [33–35].

Acknowledgements

This work was supported by the National Natural Science Foundation of China (Nos. 51603164, 51373175, 61604120), the Natural Science Basic Research Plan in Shaanxi Province of China (Nos. 2016JQ5036, No. 2017ZDJC-22), the Young Talent Fund of University Association for Science and Technology in Shaanxi, China (20170706), and the Start-up Funding for Scientific Research in Xi'an Technological University (Nos. 0853-302020350).

Electronic supplementary material: The online version of this article (https://doi.org/10.1007/s10853-017-1929-1) contains supplementary material, which is available to authorized users.

References

[1] Koetting MC, Peters JT, Steichen SD, Peppas NA (2015) Stimulus-responsive hydrogels: theory, modern advances, and applications. Mater Sci Eng R Rep 93:1–49

[2] Raeburn J, Zamith Cardoso A, Adams DJ (2013) The importance of the self-assembly process to control mechanical properties of low molecular weight hydrogels. Chem Soc Rev 42:5143–5156

[3] Kim J, Yoon J, Hayward RC (2010) Dynamic display of biomolecular patterns through an elastic creasing instability of stimuli-responsive hydrogels. Nat Mater 9:159–164

[4] Razza N, Blanchet B, Lamberti A, Pirri FC, Tulliani JM, Bozano LD, Sangermano M (2017) UV-printable and flexible humidity sensors based on conducting/insulating semi-interpenetrated polymer networks. Macromol Mater Eng 10:1700161

[5] Liu YJ, Cao WT, Ma MG, Wan P (2017) Ultrasensitive wearable soft strain sensors of conductive, self-healing, and elastic hydrogels with synergistic "soft and hard" hybrid networks. ACS Appl Mater Inter 9:25559–25570

[6] Liu S, Li L (2017) Ultra-stretchable and self-healing double network hydrogel for 3D printing and strain sensor. ACS Appl Mater Inter 9:26429–26437

[7] Gao Y, Song JF, Li SM, Elowsky C, Zhou Y, Ducharme S, Chen YM, Zhou Q, Tan L (2016) Hydrogel microphones for stealthy underwater listening. Nat Commun. https://doi.org/10.1038/ncomms12316

[8] Trung TQ, Lee N (2017) Recent progress on stretchable electronic devices with intrinsically stretchable components. Adv Mater 29:1603167

[9] Chen H, Yang F, Chen Q, Zheng J (2017) A novel design of multi-mechanoresponsive and mechanically strong hydrogels. Adv Mater 21:1606900

[10] Stuart MA, Huck WT, Genzer J, Müller M, Ober C, Stamm M, Sukhorukov GB, Szleifer I, Tsukruk VV, Urban M (2010) Emerging applications of stimuli-responsive polymer materials. Nat Mater 9:101–113

[11] Beebe DJ, Moore JS, Bauer JM, Yu Q, Liu RH, Devadoss C, Jo BH (2000) Functional hydrogel structures for autonomous flow control inside microfluidic channels. Nature 404:588–590

[12] Yashin VV, Kuksenok O, Balazs AC (2010) Modeling autonomously oscillating chemo-responsive gels. Prog Polym Sci 35:155–173

[13] Zhou H, Ding X, Zheng Z, Peng Y (2013) Self-regulated intelligent systems: where adaptive entities meet chemical oscillators. Soft Matter 9:4956–4968

[14] Yoshida R (2010) Self-oscillating gels driven by the Belousov–Zhabotinsky reaction as novel smart materials. Adv Mater 22:3463–3483

[15] Kuksenok O, Dayal P, Bhattacharya A, Yashin VV, Deb D, Chen IC, Van Vliet KJ, Balazs AC (2013) Chemo-responsive, self-oscillating gels that undergo biomimetic communication. Chem Soc Rev 42:7257–7277

[16] Zhou HW, Zheng ZH, Wang QG, Xu GH, Li J, Ding XB (2015) A modular approach to self-oscillating polymer systems driven by the Belousov–Zhabotinsky reaction. RSC Adv 5:13555–13569

[17] Yoshida R, Ueki T (2014) Evolution of self-oscillating polymer gels as autonomous polymer systems. NPG Asia Mater. https://doi.org/10.1038/am.2014.32

[18] Yoshida R, Takahashi T, Yamaguchi T, Ichijo H (1996) Self-oscillating gel. J Am Chem Soc 118:5134–5135

[19] Zhou HW, Ding XB (2016) Smart polymer materials driven by the Belousov–Zhabotinsky reaction: topological structures and biomimetic functions. Prog Chem 28:111–120

[20] Ueki T, Yoshida R (2014) Recent aspects of self-oscillating polymeric materials: designing self-oscillating polymers coupled with supramolecular chemistry and ionic liquid science. Phys Chem Chem Phys 16:10388–10397

[21] Suzuki D, Kobayashi T, Yoshida R, Hirai T (2012) Soft actuators of organized self-oscillating microgels. Soft Matter 8:11447–11449

[22] Mitsunaga R, Okeyoshi K, Yoshida R (2013) Design of a comb-type self-oscillating gel. Chem Commun 49:4935–4937

[23] Zhang Y, Zhou N, Akella S, Kuang Y, Kim D, Schwartz A, Bezpalko M, Foxman BM, Fraden S, Epstein IR, Xu DB (2013) Active cross-linkers that lead to active gels. Angew Chem Int Ed 52:11494–11498

[24] Zhou HW, Wang YR, Zheng ZH, Ding XB, Peng YX (2014) Periodic auto-active gels with topologically "polyrotaxane-interlocked" structures. Chem Commun 50:6372–6374

[25] Zhou H, Jin X, Yan B, Li X, Yang W, Ma A, Zhang X, Li P, Ding X, Chen W (2017) Mechanically robust, tough, and self-recoverable hydrogels with molecularly engineered fully flexible crosslinking structure. Macromol Mater Eng 9:1700085

[26] Lodge TP, Ueki T (2016) Mechanically tunable, readily processable ion gels by self-assembly of block copolymers in ionic liquids. Acc Chem Res 49:2107–2114

[27] Zhang Y, Zhou N, Li N, Sun MG, Kim D, Fraden S, Epstein IR, Xu B (2014) Giant volume change of active gels under continuous flow. J Am Chem Soc 136:7341–7347

[28] Sun YN, Gao GR, Du GL, Cheng YJ, Fu J (2014) Super tough, ultrastretchable, and thermoresponsive hydrogels with functionalized triblock copolymer micelles as macro-cross-linkers. ACS Macro Lett 3:496–500

[29] Zhou HW, Yang Y, Xu GH, Chen WX, Zhang WZ, Wang QG, Zheng ZH, Ding XB (2015) Ru(II)$(Tpy)_2$-functionalized hydrogels: synthesis, reversible responsiveness, and coupling with the Belousov–Zhabotinsky reaction. J Polym Sci Pol Chem 53:2214–2222

[30] Zhou H, Zheng Z, Wang Q, Xu G, Li J, Ding X (2015) A modular approach to self-oscillating polymer systems driven by the Belousov–Zhabotinsky reaction. RSC Adv 5:13555–13569

[31] Manners I (2001) Putting metals into polymers. Science 294:1664–1666

[32] Li H, Yang P, Pageni P, Tang CB (2017) Recent advances in metal-containing polymer hydrogels. Macromol Rapid Commun 14:1700109

[33] Gao J, Tang C, Smith AM, Miller AF, Saiani A (2017) Controlling self-assembling peptide hydrogel properties through network topology. Biomacromol 18:826–834

[34] Shen W, Zhang K, Kornfield JA, Tirrell DA (2006) Tuning the erosion rate of artificial protein hydrogels through control of network topology. Nat Mater 5:153–158

[35] Okumura Y, Ito K (2001) The polyrotaxane gel: a topological gel by figure-of-eight cross-links. Adv Mater 13:485–487